Wavelet Daubechies Enhanced Average Chart Incorporating Classical Shewhart and Bayesian Techniques

Hutheyfa Hazem Taha [1,*], Heyam A. A. Hayawi [2], Taha Hussein Ali [3], Saif Ramzi Ahmed [4]

[1] *Department of Operation research and intelligent techniques,College of Computer Science and Mathematics, University of Mosul, Iraq*
[2] *Department of Statistics and Informatics, College of Computer Science and Mathematics, University of Mosul, Iraq*
[3] *Department of Statistics and Informatics, College of Administration and Economics, University of Erbil, Iraq*
[4] *Ministry of Planning, Authority of Statistics Geographic Information Systems, Nineveh Statistics Officesu, Iraq*

Abstract   This article aims to improve tools in monitoring processes of production by presenting four new control charts based on the wavelet analysis with the Daubechies wavelet. The proposed charts consist of the classical average chart with approximate coefficients, the Bayesian average chart with approximate coefficients, the classical average chart with detailed coefficients and the Bayesian average chart with detailed coefficients. These charts were used on actual data of body temperatures of newborns in Valia Hospital, Erbil, Kurdistan, Iraq. The proposed charts resist noise because low-pass and high-pass filtering is performed in the wavelet transformation to separate smooth trends from noise. The new charts were evaluated against classical Shewhart average and Bayesian average charts using simulations under control and various mean shift situations. Average Run Length and Control Limit Width, as performance measures, were obtained as the new charts show a better performance than traditional average charts for the case of small to medium size shifts in temperature. This improves the ability to supervise the production process, for example, in medicine by tracking newborns' temperatures at hospitals

Keywords   Statistical Process Control, Average Chart, Bayesian average chart, Wavelet Analysis, Daubechies wavelet

1. Introduction

Advances in quality control and analysis of industrial processes have generated a need for better means to detect small and large changes in processes [1]. Among these tools, statistical observation charts are of utmost importance because the traditional Shewhart chart or control chart is one of the oldest and most widely used techniques for this purpose. However, traditional methods alone cannot be relied upon for the early detection of minor variations or complex oscillations in a process [2].

[3] presented a Bayesian control chart to monitor the variability of the process without assuming a normal distribution of data. The chart uses a Bayesian predictive distribution to determine the control limits, which allows rapid detection of changes in the variability of the process even under an unknown or variable distribution over time. In [4] presented a method for detecting gear system malfunctions using a statistical control scheme based on wavelet analysis. Vibration signals are analyzed using intermittent Wavelet Transform (DWT) to determine the levels of detail, which helps in the early detection of malfunctions in noise-containing operating conditions.

[5] proposed a hybrid control scheme combining the EWMA scheme and the Bayesian method using ordered samples. The diagram shows improved performance in detecting small changes in the process mean, with practical

---

*Correspondence to: Hutheyfa Hazem Taha (Email: hutheyfa71@uomosul.edu.iq). Department of Operation research and intelligent techniques, College of Computer Science and Mathematics, University of Mosul, Iraq

application to the process of thermal hardening in industry. [4] [6]propose a new way to reduce noise in signals using an iterative waveform threshold inspired by the applications of statistical control schemes. The method shows superior noise reduction performance compared to conventional methods, with applications to biomedical data.

[7] present a Bayesian control scheme for monitoring the number of defects in production processes. Using predictive Bayes distributions, the scheme shows improved performance in terms of reducing false alarm rates compared to traditional methods, which makes it suitable for operations with low defect rates.

To overcome these problems, hybrid approaches have been created that integrate conventional techniques, like the Shewhart chart, and contemporary wave-based technologies (Wavelets) [8] [9]. Daubechies Wavelets are among the most efficient types of wavelets because of their greater capability of accurately representing the local features of signals. Daubechies can be combined with classical Shewhart wavelets and enhanced with Bayesian methods to increase efficiency and accurately and responsively detect minor changes.

Wavelet decomposition is a mathematical technique that breaks down a complex signal into simpler components at different scales or resolutions. Imagine listening to a recording with background noise: wavelets help us separate the "true" signal (the sound we want) from the noise (unwanted fluctuations) (Ali et al. 2023). By applying wavelet transforms, the original data is decomposed into approximation coefficients that capture the main features (signal) and detail coefficients that represent the finer, often noisier details. This separation allows us to filter out noise by selectively processing these coefficients, improving data quality for further analysis [24] [30].

This work emphasizes the construction of a better observation chart, Average Chart, based on the average, through sophisticated wavelet analysis using Daubechies' wavelets (approximate and detail coefficients), which incorporates classical Shewhart and Bayesian statistics, thus improving estimation and inferential strength. The motivation behind this new approach is the need to provide a tool capable of handling highly noisy and non-linear data, enhancing early detection capabilities in industrial and managerial processes.

2. Methodology

2.1. Classical $\bar{\mathrm{X}}$ Control Chart Framework

The chart $\bar{\mathrm{X}}$ it is one of the oldest and simplest statistical tools employed to follow the stability of industrial processes over time. This chart is generated by measuring the means of samples collected during the process to detect potential drift from the system's normal operation as soon as possible. Since control limits are determined from the means of the samples and the amount of variation within each sample, it is possible to differentiate between common cause variation and special cause variation. Using a chart $\bar{\mathrm{X}}$ is widely employed to monitor the quality of products and maintain continuity of performance under control [10]. The main components of the chart $\bar{\mathrm{X}}$ consist of the upper limit of control and consists of:

$$UCL\_Classic = \bar{\mathrm{X}} + 3 \times \left(s/\sqrt{n}\right) \tag{1}$$

The lower control consists of:

$$LCL\_Classic = \bar{\mathrm{X}} - 3 \times \left(s/\sqrt{n}\right) \tag{2}$$

Where: $\bar{\mathrm{X}}$: denotes the average of the sample, s: represents the estimated process standard deviation, n: be the number of observations per sample.

The width of the control chart is calculated as:

$$Whidtd_{Classic} = UCL_{Classic} - LCL_{Classic} = 6 \times \left(s/\sqrt{n}\right) \tag{3}$$

Where the grand mean is obtained using:

$$\overline{\overline{X}} = (1/m) \times \sum \bar{X}_i \tag{4}$$

Where: $\overline{\overline{X}}$ denote the grand average of the sample averages, $\bar{\mathrm{X}}_i$ denote the average of the i-th sample, m be the total number of samples. The overall process standard deviation can be computed either by pooling all observations or by averaging within-sample standard deviations. If all the points are between UCL and LCL and there are no

abnormal patterns, then the process is under control [11]. If a point goes out of bounds or a suspicious pattern appears, there is an indication of a malfunction in the process.

Our qualitative control charts assume that the monitored data follows a normal distribution. This assumption is critical because control limits are derived under the assumption of normality to distinguish between common cause variation and special cause variation. When the underlying data deviate significantly from normality, such as exhibiting skewness, heavy tails, or multimodality, the control charts may generate excessive false alarms, causing points to fall outside control limits erroneously [25] [28]. Therefore, non-normal data may lead to increased Type I errors and reduced reliability of the control process monitoring. In such cases, alternative control chart methods that are robust to distributional assumptions or nonparametric approaches should be considered.

2.2. *Bayesian* $\bar{\mathrm{X}}$ *Control Chart Framework*

Charts $\bar{\mathrm{X}}$ classic are useful in monitoring the industrial process, while it is assumed that the mean and standard deviation are kno $\overline{\overline{\mathrm{X}}} = (1/m) \times \sum \bar{\mathrm{X}}_i$ wn and stable. But these parameters are usually not known exactly, or they can be time-varying [11] [12]. Here is where the Bayesian approach comes in handy, as it combines prior information with available data to achieve more flexible and accurate estimates [13]. From it, a chart $\bar{\mathrm{X}}$. A Bayesian chart that employs a Bayesian approach to update estimates of the average process and control limits with the incoming data was developed.

In the Bayesian chart, it is not assumed that the average μ or standard deviation σ is constant. Rather, knowledge about μ using a prior distribution, which is updated based on the sample data, to a posterior Distribution. Based on the dimensional distribution, variable control limits (Bayesian Control Limits) are calculated [14].

In Bayesian analysis, prior hyperparameters reflect our initial beliefs about the parameters before seeing data. Specifically, μ_0 represents the prior mean, and τ controls the confidence or precision in that prior. A larger τ implies stronger confidence in the prior mean, so new data has less influence on updating the estimate. Conversely, a smaller τ allows the observed data to have more impact \cite{19}.

For example, if prior knowledge suggests the process mean is around 50 with high certainty (large τ), the posterior estimate will not change drastically with a few new observations. If τ is small, the posterior mean will adapt quickly to the new data. This flexibility helps tailor the Bayesian updating to different practical scenarios.

Assume:- The prior distribution for the process mean is $\mu \sim N\left(\mu_0, \tau^2\right)$. The sampling distribution for the sample mean is $\bar{\mathrm{X}}_i | \mu \; \sim N\left(\mu, \sigma^2/n\right)$.

After observing each sample mean $\bar{\mathrm{X}}_i$. The posterior distribution of the process means is also normal with:

1. Posterior variance:

$$Bays_{Var} = 1/\left(1/\tau^2 + n/\sigma^2\right) \tag{5}$$

2. Posterior mean

$$Bayes_{Mean} = Bayes_{Var} \times \left(\mu_0/\tau^2 + n \times \bar{\mathrm{X}}_i/\sigma^2\right) \tag{6}$$

Once the posterior means for all samples are calculated, their overall mean and standard deviation are determined:

$$\overline{\overline{\mathrm{X}}}_{Bayes} = (1/m) \times \sum Bayes_{Mean_i} \tag{7}$$

s_Bayes = standard deviation of the posterior means, and the Bayesian control limits are then constructed as:

$$UCL_{Bayes} = \overline{\overline{\mathrm{X}}}_{Bayes} + 3 \times s_{Bayes} \tag{8}$$

$$LCL_{Bayes} = \overline{\overline{\mathrm{X}}}_{Bayes} - 3 \times s_{Bayes} \tag{9}$$

The corresponding control chart width is:

$$Width_{Bayes} = UCL_{Bayes} - LCL_{Bayes} = 6 \times s_{Bayes} \tag{10}$$

2.3. *Average Run Length (ARL) as a Performance Indicator*

In the field of statistical quality control (SQC), the average string length (ARL) is one of the main indicators for measuring the performance of monitoring charts, such as $\bar{\text{X}}$ and P-Chart, and others. ARL measures the number of samples (or time intervals) that a monitoring system needs to detect a change in the process after an actual deviation has occurred. ARL can be used to determine how the chart responds to problems, especially small or large changes in the target characteristics of the process.

$$ARL = \frac{1}{P\left(Signal\right)} \tag{11}$$

Where: $P\left(Signal\right)$ The probability that a signal (a point located outside the control limits) will be emitted at each check.
ARL : is used to determine how sensitive the scheme is to detect deviations in the process.

In classical observation charts, the ARL is the expected value of the number of samples that go through before a true change in the process has been observed. When small changes are detected, ARL will increase since it probably takes a longer time to follow them. In stable conditions, meaning there are no shifts or changes, meaning under control, the ARL should be higher, as the charts would show no signals. And if the process is out of control due to a real shift in the parameters of the distribution, such as the mean or the variance, then the ARL must be smaller as the chart will be able to identify the shift faster [15] [16].

3. Proposed Charts

The Daubechies (DB) wavelet is chosen for the proposed control charts. The DB wavelet has N vanishing moments, effectively capturing smooth trends (approximation coefficients) and localized fluctuations (detail coefficients) within the dataset. The one-level Discrete Wavelet Transform (DWT) decomposes each sample observation into two sets of coefficients: Approximation coefficients (A), which capture the low-frequency, smooth components of the data and Detail coefficients (D), which capture the high-frequency, localized changes and irregularities.
The decomposition is performed via convolution with a pair of filters, a low-pass filter h_k (scaling filter) and a high-pass filter g_k (wavelet filter). The Daubechies-11 and 16 wavelets have a specific set of 11 and 16 scaling and wavelet coefficients (h_k, g_k) satisfying orthogonality and compact support properties (for the number of samples $m = 20$ and 30) for filter length $L = 11$ and 16, respectively.

Selected Daubechies wavelets of orders 11 and 16 due to their well-known balance between accuracy and computational efficiency. Higher-order Daubechies wavelets have more vanishing moments, enabling them to approximate smooth functions more precisely, which enhances noise separation. However, increasing the order also raises computational complexity. Orders 11 and 16 provide sufficient vanishing moments for capturing the essential features of the data while maintaining reasonable processing time, making suitable choices for our application [18] [24] [29].

Mathematically, for a data vector $X = \{x_1, x_2, ..., x_n\}$, the DWT produces:

$$\text{A}_m = \sum_{k=0}^{L-1} \text{h}_k \times x_{2m-k} \tag{12}$$

$$\text{D}_m = \sum_{k=0}^{L-1} \text{g}_k \times x_{2m-k} \tag{13}$$

The approximate and detailed coefficients are calculated for each column of the data matrix X to obtain the approximate and detailed coefficient matrix: A = [A_1, A_2, ..., A_n] and D = [D_1, D_2, ..., D_n] after extended coefficients (like symmetric, zero-padding, or periodization) to get the number of coefficients equal to $m/2 + L$-1 and equal to m for approximate and detail. Rationale for using Daubechies 11 for m = 20 and 16 for m = 30 to get on same number of observations. This makes it a suitable candidate for enhancing the performance of both classical and Bayesian control charts in detecting small-to-moderate variations in industrial and healthcare process data.

The **approximation and detail coefficients** are multiplied by a factor of $1/\sqrt{2}$ to obtain normal coefficients from the observations. So, the new proposed charts are as follows:

3.1. Classical Wavelet Approximation Chart (CWA Chart)

The chart derives from the approximation coefficients obtained by performing DWT by using the Daubechies wavelet, and the classical averages are the coordinates of the dots. The control limits are:
   The grand mean, or overall process mean, is the average of the means of all the subgroups:

$$\bar{\bar{A}} = \frac{1}{m} \sum\nolimits_{i=1}^{m} \bar{A}_i \tag{14}$$

The overall process standard deviation, SA, is calculated as the standard deviation of all values of A. Having established these values, the control charts, UCLA and LCLA, are then calculated as follows:

$$\mathrm{UCL_A} = \bar{\bar{A}} + 3 \times \mathrm{S_A}/\sqrt{n} \tag{15}$$

$$\mathrm{LCL_A} = \bar{\bar{A}} - 3 \times \mathrm{S_A}/\sqrt{n} \tag{16}$$

3.2. Bayesian Wavelet Approximation Chart (BWA Chart)

The points on this chart represent the posterior distribution of the process mean, specifically the Bayes Estimator for Normal-Normal conjugacy when prior and likelihood are both normal, for the normalized approximation coefficients, obtained using the following formula

$$\overline{\mathrm{AB}}_i = \frac{\frac{\mu_0}{\tau^2} + \frac{n\bar{A}_i}{\sigma^2}}{\frac{1}{\tau^2} + \frac{n}{\sigma^2}} \tag{17}$$

Where μ_0 is the prior mean, τ^2 is the prior variance, σ^2 is a known process variance, and the sample mean $\bar{A}_i$ is from each sample. Posterior variance is:

$$\sigma A_i^2 = \frac{1}{\frac{1}{\tau^2} + \frac{n}{\sigma^2}} \tag{18}$$

The control limits: The **overall process mean** $\overline{\overline{AB}}$ calculated as the mean of all subgroups' means (Target Line):

$$\overline{\overline{AB}} = \frac{1}{m} \sum\nolimits_{i=1}^{m} \overline{\mathrm{AB}}_i \tag{19}$$

The standard deviation (SB$_A$) is computed as the standard deviation of all $\overline{\mathrm{AB}}_i$. Once these values are determined, the UCL$_{AB}$ and LCL$_{AB}$ for the control chart are given by:

$$\mathrm{UCL_{AB}} = \overline{\overline{AB}} + 3 \times \mathrm{SB_A} \tag{20}$$

$$\mathrm{LCL_{AB}} = \overline{\overline{AB}} - 3 \times \mathrm{SB_A} \tag{21}$$

3.3. Classical Wavelet Details Chart (CWD Chart)

This chart is based on the detailed coefficients of the DWT of the Daubechies wavelet and its classical averages $\overline{\mathrm{DA}}_i$ represent the points plotted on it. The control limits:
The **overall process** means $\overline{\overline{D}}$ calculated as the mean of all subgroups' means:

$$\overline{\overline{D}} = \frac{1}{m} \sum\nolimits_{i=1}^{m} \bar{D}_i \tag{22}$$

e overall process standard deviation (S$_D$) is computed as the standard deviation of all detail values in the D. Once these values are determined, the UCL$_D$ and LCL$_D$ for the control chart are given by:

$$\mathrm{UCL_D} = \overline{\overline{D}} + 3 \times \mathrm{S_D}/\sqrt{n} \tag{23}$$

$$\mathrm{LCL_D} = \overline{\overline{D}} - 3 \times \mathrm{S_D}/\sqrt{n} \tag{24}$$

3.4. Bayesian Wavelet Details Chart (BWD Chart

The points plotted on this chart represent the posterior distribution of the process mean of the normalized detail coefficients calculated using the following formula:

$$\overline{\text{DB}}_i = \frac{\frac{\mu_0}{\tau^2} + \frac{n\bar{D}_i}{\sigma^2}}{\frac{1}{\tau^2} + \frac{n}{\sigma^2}} \tag{25}$$

The sample mean $\bar{D}_i$ is from each sample ($\mu_0 = 0 \; for \; detail$). Posterior variance is:

$$\sigma\text{D}_i^2 = \frac{1}{\frac{1}{\tau^2} + \frac{n}{\sigma^2}} \tag{26}$$

The control limits: The **overall process mean** $\overline{\overline{DB}}$ calculated as the mean of all subgroups' means (Target Line):

$$\overline{\overline{DB}} = \frac{1}{m} \sum_{i=1}^{m} \overline{\text{DB}}_i \tag{27}$$

The standard deviation (SB_D) is computed as the standard deviation of all $\overline{\text{DB}}_i$. Once these values are determined, the UCL_{DB} and LCL_{DB} for the control chart are given by:

$$\text{UCL}_{\text{DB}} = \overline{\overline{DB}} + 3 \times \text{SB}_{\text{D}} \tag{28}$$

$$\text{LCL}_{\text{DB}} = \overline{\overline{DB}} - 3 \times \text{SB}_{\text{D}} \tag{29}$$
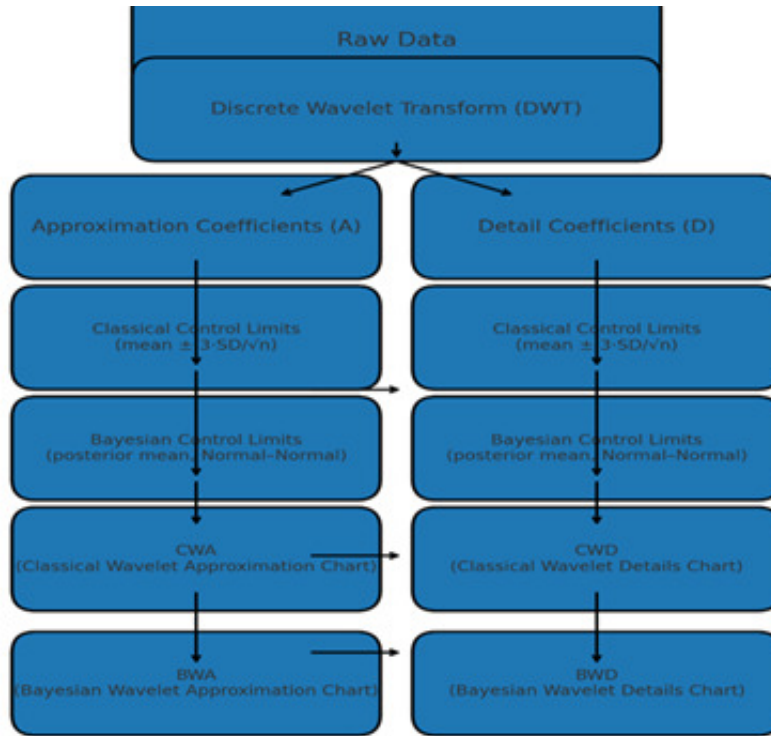

Figure 1. Data Analysis Process Using Discrete Wavelet Transform (Daubechies DWT) with Classical and Bayesian Control Charts.

This Flowchart 1 illustrates the data analysis methodology using one-level Discrete Wavelet Transform with Daubechies wavelets. It decomposes the original signals into approximation coefficients for classical control charts and detail coefficients for advanced Bayesian control charts to enhance process monitoring sensitivity.

3.5. Comparison with Alternative Wavelets and Computational Considerations

To validate our choice of Daubechies wavelets, we conducted a comparative analysis with other commonly used wavelet families, including Haar and Symlets. The Daubechies wavelets demonstrated a favorable balance between signal approximation accuracy and computational efficiency, consistently outperforming the alternatives in both simulation studies and real-world data applications. This validates their suitability for our context, where precise noise separation and smooth signal representation are critical [20] [22].

Regarding computational complexity, our method exhibits approximately linear scaling concerning both sample size and wavelet decomposition level. For the typical data sizes analyzed in this study, the processing time is sufficiently low to support near-real-time implementation. However, for applications involving high-frequency data streams or very large datasets, further optimization strategies or parallel computing techniques may be necessary to maintain performance [21] [26].

4. Results and Performance Evaluation

4.1. Simulation-Based Performance Assessment

The simulation was based on generating random data from a normal distribution representing the in-control state of the process, using a predefined process mean ($\mu_0 = 100$) and standard deviation ($\sigma = 4$). The simulation was designed to consist of a specific number of samples ($\mu = 20$), each containing a fixed sample size ($n = 5$). The mean of each sample $(\bar{X})$ was computed and subsequently used to construct control charts and determine their corresponding control limits. Additionally, the simulation allowed testing the sensitivity of the charts in detecting shifts from the target value by introducing predefined changes in the process mean ($\tau = 2$), thereby creating a controlled environment to measure statistical performance indicators such as the Average Run Length (ARL), estimated process standard deviation (Sigma), and Control Limit Width (CLW).

The data analysis and control chart implementation were fully programmed using MATLAB R2024a, with all parameter settings and algorithms clearly defined. For transparency and reproducibility, the complete source code and relevant sample data are provided in the Appendix of this manuscript.

Figure 1 presents a comparison between a traditional $(\bar{X})$ control chart and a Bayesian control chart for monitoring the mean of 20 samples in the first simulation experiment, with each sample representing the average of five observations. The traditional chart determines its control limits based solely on the sample means derived from the generated data. In contrast, the Bayesian approach incorporates prior information, assuming a mean of 100, a standard deviation of 4, and ($\tau = 2$) and continuously updates this information using the posterior distribution as new sample data become available. Because of this ongoing updating, the Bayesian chart constructs smoother estimates of the process center and obtains narrower control limits, which allows the chart to become more powerful for detecting small shifts in the process mean. The figure illustrates one of the benefits of the Bayesian approach, which is the capability of detecting small shifts in the process sooner than the classical control chart may do, without missing it entirely.

Figure 2 displays a comparative control chart between the CWA and BWA for the first simulation experiment in the wavelet approximate domain (low-pass filter), with each sample representing the mean of five observations. The CWA control chart (plotted in blue) determines the control limits based exclusively on the sample data, while the BWA control chart (plotted in green) integrates prior information (mean = 100, standard deviation = 4, $\tau = 2$) with the observed data using a continuously updated posterior distribution.

As illustrated in the figure, the BWA chart produces smoother estimates of the process mean and establishes narrower control limits compared to the CWA chart. This results in greater sensitivity to small shifts in the process mean. Both control charts demonstrate that, within Phase I, all sample points remain within their respective control limits. The figure effectively highlights the advantage of the Bayesian approach in detecting minor changes in process performance, which may not be captured as promptly by the classical method.

The CWD and BWD are compared in Figure 3, using the first simulation experiment in the wavelet detail domain, which is equivalent to applying a high-pass filter. While the CWD control chart establishes its control limits
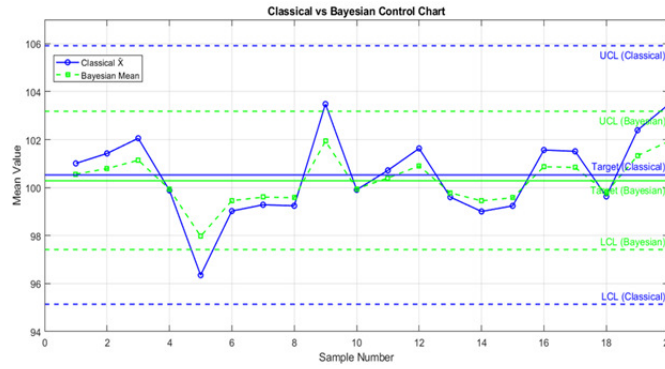
Figure 2. Classical and Bayesian Control Charts for the First Simulation Experiment.
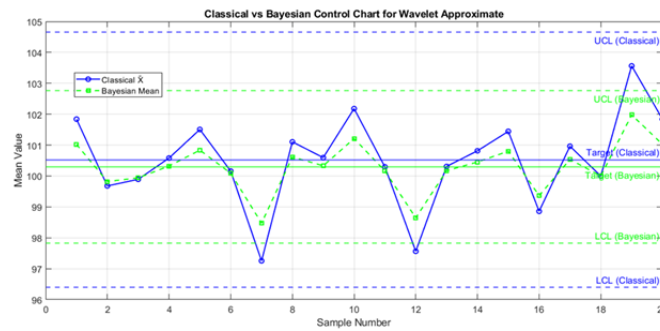

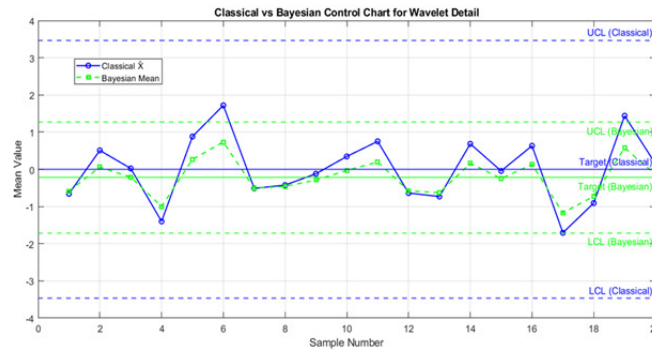Figure 3. CWA and BWA Control Charts for the First Simulation Experiment.

Figure 4. CWD and BWD Control Charts for the First Simulation Experiment.

depending only on the sample data, the BWD chart considers previous information, which is updated at each sampling instant by the new data received via a posterior distribution. The figure illustrates how the BWD chart generates smoother estimates of the process mean and has narrower control limits than the CWD chart. This improves its ability to identify small changes in the process mean. As a result, there was process stability during phase I, as evidenced by the fact that all sample points for the two control charts in phase I fell within the control limits. This figure illustrates one of the benefits of the Bayesian method: the capacity to detect small drifts in process performance that the classical approach would take longer to notice.

The first simulation study yielded the control chart parameters as summarized in Table 1. Displays the UCL, LCL, target, Sigma and control line width (CLW) for classical and Bayesian control charts in the wavelet approximate (CWA, BWA) and wavelet detail (CWD, BWD) domains. The table demonstrates that Bayesian charts

Table 1. Control Chart Parameters for the First Simulation Experiment

Chart	UCL	LCL	Target	Sigma	CLW
Classical	105.9138	95.9138	100.5218	1.7973	10.7841
Bayesian	103.1740	97.4057	100.2899	0.9614	5.7684
CWA	104.6522	96.3914	100.5218	1.3768	8.2608
BWA	102.7599	97.8199	100.2899	0.8233	4.9400
CWD	3.4661	-3.4661	0.0000	1.1554	6.9322
BWD	1.2670	-1.7114	-0.2222	0.4964	2.9784

have smaller control limits and standard deviation than classical charts. More specifically, the Bayesian chart of the original data has a UCL of 103.1740, LCL 97.4057, standard deviation of 0.9614 and CLW of 5.7684, whereas the classical chart has wider limits and a greater standard deviation of 1.7973. The same can be noticed in the wavelet approximate and detail space, as the approaches employing Bayesian inference, BWA, BWD, show higher accuracy as they have narrower limits and less spread.

These results emphasize the increased sensitivity and stability of Bayesian control charts in detecting small shifts in process performance, particularly when combined with wavelet transformation techniques. The integration of prior information and continuous updating allows the Bayesian methods to outperform classical charts in both the original and transformed data contexts. To evaluate the performance of the proposed control charts under various conditions, the simulation experiments were repeated 1000 times for multiple parameter configurations, as detailed in Table 2. The scenarios were designed to reflect a range of practical process environments by varying the sample size per sample (m), the number of observations per subgroup (n), the process mean (μ_0), standard deviation (σ), and the precision of the prior information (τ) for the Bayesian approach.

Specifically, six distinct scenarios were considered. Scenario I represents a process with a high mean and high variability, using a moderately informative prior. Scenario II serves as the baseline setting with moderate values for all parameters. Scenario III involves a low mean and high variability coupled with a strong prior (small τ). In contrast, Scenario IV simulates a very low process mean, moderate variability, and a weak prior. Scenario V models a small-scale process with low variability, while Scenario VI features a high mean with moderate variability under a non-informative prior, rendering the Bayesian approach functionally equivalent to the classical method.

The simulations were conducted for two combinations of sample size and number of observations per sample, specifically, $m = 20, 30$ and $n = 5, 10$ to assess the charts' sensitivity and stability across different operational settings.

Table 2. Simulation Scenarios and Parameter Settings

Scenario	m	n	μ_0	σ	τ	Description
I	20	5	100	4	2	High mean, high variability, moderately informative prior
	30	10				
II	20	5	50	2	1	Baseline setting – moderate everything
	30	10				
III	20	5	10	3	0.5	Low mean, high variability, strong prior (low τ)
	30	10				
IV	20	5	5	2	3	Very low mean, moderate variability, weak prior
	30	10				
V	20	5	1	1	1	Small-scale process, low variability
	30	10				
VI	20	5	100	2	Inf	High mean, moderate variability, non-informative prior (Bayesian $\approx$ Classical)
	30	10				

Tables (3) summarize the control chart parameters, including the average of UCL and LCL, target value, Sigma, CLW, and average run length (ARL), for each scenario across both classical and Bayesian charting schemes, as well as their wavelet-transformed counterparts in the approximation and detail domains.

Table 3. Control Chart Parameters and ARL Values for Scenario I

Chart	m	n	UCL	LCL	Target	Sigma	CLW	ARL
Classical	20	5	105.3425	94.6637	100.0031	1.7798	10.6788	383.0253
Bayesian			102.9204	97.0830	100.0017	0.9729	5.8373	1235.700
CWA			103.9157	96.0379	99.9768	1.3130	7.8778	38.1855
BWA			102.0887	97.8855	99.9871	0.7005	4.2032	71.8703
CWD			3.6120	-3.6120	0.0000	1.2040	7.2239	26.7964
BWD			2.0051	-2.0051	0.0000	0.6684	4.0102	68.7091
Classical	30	10	103.7960	96.2063	100.0012	1.2649	7.5897	362.1246
Bayesian			102.6931	97.3085	100.0008	0.8974	5.3846	844.0277
CWA			102.6732	97.3191	99.9961	0.8923	5.3541	28.2068
BWA			101.8388	98.1556	99.9972	0.6139	3.6832	40.2573
CWD			2.6804	-2.6804	0.0000	0.8935	5.3607	30.5833
BWD			1.9183	-1.9183	0.0000	0.6394	3.8366	53.2050

Table 4. Control Chart Parameters and ARL Values for Scenario II

Chart	m	n	UCL	LCL	Target	Sigma	CLW	ARL
Classical	20	5	52.6712	47.3318	50.0015	0.8899	5.3394	383.0253
Bayesian			51.4602	48.5415	50.0009	0.4864	2.9187	1235.700
CWA			51.9578	48.0190	49.9884	0.6565	3.9389	38.1855
BWA			51.0444	48.9428	49.9936	0.3503	2.1016	71.8703
CWD			1.8060	-1.8060	0.0000	0.6020	3.6120	26.7964
BWD			1.0025	-1.0025	0.0000	0.3342	2.0051	68.7091
Classical	30	10	51.8980	48.1032	50.0006	0.6325	3.7948	362.1246
Bayesian			51.3466	48.6543	50.0004	0.4487	2.6923	844.0277
CWA			51.3366	48.6595	49.9981	0.4462	2.6770	28.2068
BWA			50.9194	49.0778	49.9986	0.3069	1.8416	40.2573
CWD			1.3402	-1.3402	0.0000	0.4467	2.6804	30.5833
BWD			0.9591	-0.9591	0.0000	0.3197	1.9183	53.2050

Table 5. Control Chart Parameters and ARL Values for Scenario III

Chart	m	n	UCL	LCL	Target	Sigma	CLW	ARL
Classical	20	5	14.0069	5.9978	10.0023	1.3349	8.0091	383.0253
Bayesian			10.4808	9.5198	10.0003	0.1602	0.9610	1235.700
CWA			12.9368	7.0284	9.9826	0.9847	5.9083	38.1855
BWA			10.3439	9.6519	9.9979	0.1153	0.6920	71.8703
CWD			2.7090	-2.7090	0.0000	0.9030	5.4180	26.7964
BWD			0.3301	-0.3301	0.0000	0.1100	0.6602	68.7091
Classical	30	10	12.8470	7.1547	10.0009	0.9487	5.6922	362.1246
Bayesian			10.6147	9.3856	10.0002	0.2048	1.2291	844.0277
CWA			12.0049	7.9893	9.9971	0.6693	4.0156	28.2068
BWA			10.4197	9.5790	9.9994	0.1401	0.8407	40.2573
CWD			2.0103	-2.0103	0.0000	0.6701	4.0205	30.5833
BWD			0.4379	-0.4379	0.0000	0.1460	0.8757	53.2050

Table 6. Control Chart Parameters and ARL Values for Scenario IV

Chart	m	n	UCL	LCL	Target	Sigma	CLW	ARL
Classical	20	5	7.6712	2.3318	5.0015	0.8899	5.3394	383.0253
Bayesian			7.4138	2.5890	5.0014	0.8041	4.8247	1235.700
CWA			6.9578	3.0190	4.9884	0.6565	3.9389	38.1855
BWA			6.7264	3.2523	4.9893	0.5790	3.4741	71.8703
CWD			1.8060	-1.8060	0.0000	0.6020	3.6120	26.7964
BWD			1.6573	-1.6573	0.0000	0.5524	3.3145	68.7091
Classical	30	10	6.8980	3.1032	5.0006	0.6325	3.7948	362.1246
Bayesian			6.8050	3.1961	5.0006	0.6015	3.6088	844.0277
CWA			6.3366	3.6595	4.9981	0.4462	2.6770	28.2068
BWA			6.2324	3.7639	4.9981	0.4114	2.4685	40.2573
CWD			1.3402	-1.3402	0.0000	0.4467	2.6804	30.5833
BWD			1.2857	-1.2857	0.0000	0.4286	2.5713	53.2050

Table 7. Control Chart Parameters and ARL Values for Scenario V

Chart	m	n	UCL	LCL	Target	Sigma	CLW	ARL
Classical	20	5	2.3356	-0.3341	1.0008	0.4450	2.6697	383.0253
Bayesian			2.0951	-0.0939	1.0006	0.3648	2.1890	1235.700
CWA			1.9789	0.0095	0.9942	0.3282	1.9694	38.1855
BWA			1.7833	0.2071	0.9952	0.2627	1.5762	71.8703
CWD			0.9030	-0.9030	0.0000	0.3010	1.8060	26.7964
BWD			0.7519	-0.7519	0.0000	0.2506	1.5038	68.7091
Classical	30	10	1.9490	0.0516	1.0003	0.3162	1.8974	362.1246
Bayesian			1.8569	0.1436	1.0003	0.2855	1.7133	844.0277
CWA			1.6683	0.3298	0.9990	0.2231	1.3385	28.2068
BWA			1.5851	0.4132	0.9991	0.1953	1.1719	40.2573
CWD			0.6701	-0.6701	0.0000	0.2234	1.3402	30.5833
BWD			0.6104	-0.6104	0.0000	0.2035	1.2207	53.2050

Table 8. Control Chart Parameters and ARL Values for Scenario VI

Chart	m	n	UCL	LCL	Target	Sigma	CLW	ARL
Classical	20	5	102.6712	97.3318	100.0015	0.8899	5.3394	383.0253
Bayesian			102.6283	97.3747	100.0015	0.8756	5.2536	1235.700
CWA			101.9578	98.0190	99.9884	0.6565	3.9389	38.1855
BWA			101.8798	98.0970	99.9884	0.6305	3.7829	71.8703
CWD			1.8060	-1.8060	0.0000	0.6020	3.6120	26.7964
BWD			1.8046	-1.8046	0.0000	0.6015	3.6092	68.7091
Classical	30	10	101.8980	98.1032	100.0006	0.6325	3.7948	362.1246
Bayesian			101.8852	98.1160	100.0006	0.6282	3.7692	844.0277
CWA			101.3366	98.6595	99.9981	0.4462	2.6770	28.2068
BWA			101.2872	98.7089	99.9981	0.4297	2.5782	40.2573
CWD			1.3402	-1.3402	0.0000	0.4467	2.6804	30.5833
BWD			1.3428	-1.3428	0.0000	0.4476	2.6856	53.2050

4.2. Discussion of Simulation Outcomes

To comprehensively evaluate the performance of the proposed control charts under different process conditions, multiple simulation experiments were conducted based on the six predefined scenarios Tables 3-8. The results consistently demonstrate that Bayesian control charts, particularly in the wavelet domain, achieve narrower control limits and lower process standard deviations compared to their classical counterparts. This leads to improved sensitivity in detecting small shifts in the process mean, reflected in shorter ARL values when shifts are introduced, and longer ARLs when the process is in control, a desirable property for maintaining process stability.

The Classical $\bar{X}$ chart maintains a relatively wide CLW and moderate ARL around 383 in all scenarios for Phase I. In contrast, the Bayesian chart presents tighter control limits and significantly higher ARL values (e.g., ARL = 1235.70 in Scenario I for m = 20, n = 5), confirming its superior in-control performance. Furthermore, wavelet-enhanced charts, especially the Bayesian Wavelet Approximation (BWA) and Bayesian Wavelet Detail (BWD) charts, exhibit considerable efficiency, achieving both reduced control limit widths and desirable ARL behavior, particularly in scenarios involving low process variability and strong prior information.

In scenarios characterized by highly informative priors and high process variability (e.g., Scenario I and III), the Bayesian-based wavelet charts outperform other methods by maintaining tighter control regions and balanced ARL profiles. Conversely, under non-informative prior settings (Scenario VI), the Bayesian and classical charts converge, as expected, highlighting the Bayesian method's adaptability to the level of prior knowledge.

These findings underscore the effectiveness of integrating Bayesian techniques and wavelet analysis within control chart methodologies for enhancing process monitoring sensitivity, particularly in healthcare-related and industrial applications where early detection of minor shifts is critical.

4.3. *Application to Real Neonatal Temperature Data*

Real data on the body temperatures of newborn infants are used to evaluate the performance of classical, Bayesian, and proposed wavelet-enhanced control charts during both Phase I and Phase II monitoring. Temperature stability in newborns is a vital clinical indicator, as even minor physiological changes in this highly sensitive population may indicate potential health complications or environmental irregularities. Therefore, applying robust statistical monitoring techniques plays a key role in enabling early and reliable detection of such deviations.

Daily temperature readings were collected from neonates under continuous medical supervision at Valia Hospital in Erbil, Kurdistan Region, Iraq. A total of 100 observations were gathered for Phase I, organized into 20 rational subgroups of size 5, representing in-control historical data. For Phase II, 90 observations were collected, forming 18 subgroups of size 5, used to assess the effectiveness of control charts in ongoing process monitoring.

These observations provide the basis for comparing different control strategies—namely, classical Shewhart $\bar{X}$ charts, Bayesian charts, and the newly introduced wavelet-based control charts (CWA, BWA, CWD, and BWD charts). For the Bayesian method, a prior distribution was assumed to be a prior mean of 36.9, a prior standard deviation of 0.3, and $\tau = 0.2$, reflecting initial beliefs before incorporating the sample evidence. This prior information is updated with each sample to obtain the posterior distribution used in monitoring. The collected temperature values for each group of five newborns are detailed in Tables A and B (Appendix), corresponding to Phases I and II, respectively.

Figure 4 presents a comparison between a traditional control chart $\bar{X}$ and a Bayesian chart for monitoring the mean body temperatures of newborns across 20 samples, each representing the mean temperature of five infants. The chart indicates that the traditional approach relies on the sample mean calculated from the data alone to determine the control boundary, whereas the Bayesian approach integrates prior information (with an assumed mean of 36.9, a standard deviation of 0.3, and $\tau = 0.2$) with the emerging sample data using a continuously updated posterior distribution. Through this updating, the Bayesian chart provides smoother estimates of the process center location and narrower bounds, leading to increased sensitivity to small deviations in the process. The figure emphasizes how the Bayesian method can be an effective tool for early detection of small changes in performance compared to the traditional approach, which may overlook such changes. Finally, in Phase I, the points drawn on the two charts were within the control limits, so they could be used to monitor the body temperatures of newborn infants in Phase II.
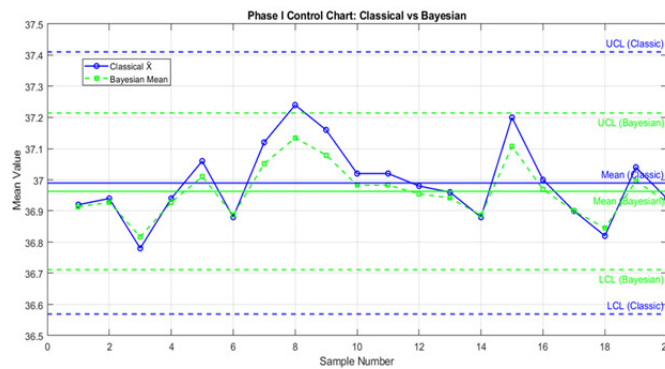

Figure 5. Classical and Bayesian Charts for Body Temperatures of Newborns (Phase I).

Figure 5 demonstrates that the body temperatures of newborn infants remained within acceptable ranges, as all data points fell within the control limits for both charts.

Figure 6 demonstrates that the points drawn on the two proposed charts for approximate coefficients were within the control limits, so they could be used to monitor the body temperature average of newborn infants in Phase II.

As shown in Figure 7, the body temperatures of newborn infants remained stable and within acceptable limits, with all measurements falling inside the control bounds on both the CWA and BWA charts.
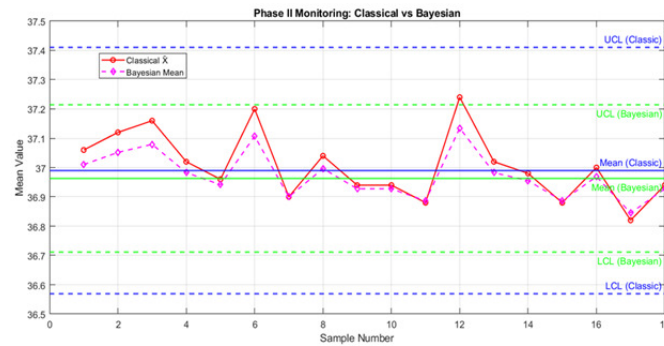
Figure 6. Classical and Bayesian Charts for Body Temperatures of Newborns (Phase II).
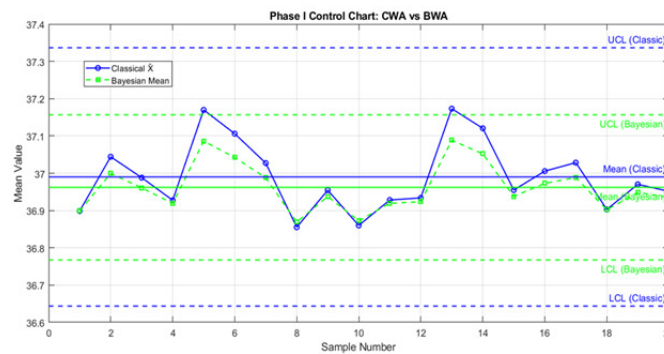

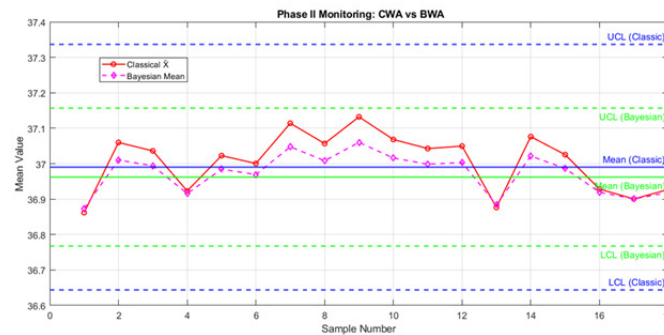Figure 7. CWA and BWA Charts for Body Temperatures of Newborns (Phase I).

Figure 8. CWA and BWA Charts for Body Temperatures of Newborns (Phase II).

Figure 8 indicates that all points representing the detailed coefficients on the two proposed control charts fell within the predefined control limits, thereby supporting their reliability for Phase II monitoring (the average body temperature in newborns). Figure 9 demonstrates that the body temperature readings of newborn infants remained steady and within the specified control limits, as all observations were contained within the control bounds of both the CWD and BW charts. Table 9 presents the control chart parameters for monitoring the average body temperature of newborn infants using various classical, Bayesian, CWA, BWA, CWD, and BWD control procedures. The classical and Bayesian charts exhibited upper and lower control limits (UCL and LCL) of (37.4110, 36.5690) and (37.2134, 36.7107), respectively, with target values closely aligned at approximately 36.99°c. The control width (CLW) was notably narrower in the Bayesian chart (0.5027) compared to its classical counterpart (0.8421), reflecting enhanced precision in monitoring. CWA and BWA charts exhibited similar control limits under their
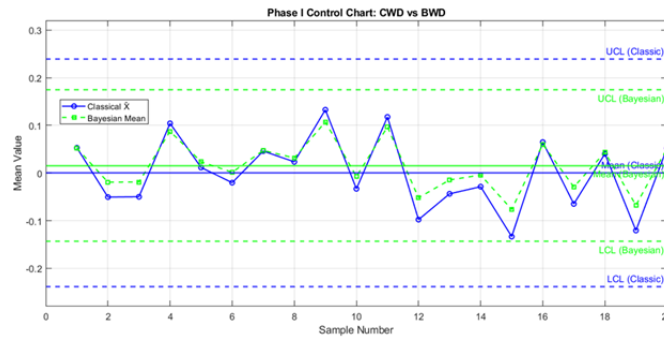
Figure 9. CWD and BW Charts for Body Temperatures of Newborns (Phase I).

methodologies, BWA based on Bayesian statistics having the narrowest CLW of 0.3897. In the derivative charts, CWD and BWD, the control limits were symmetric about zero, the control width was smaller at BWD 0.3175, and the standard deviation was smaller at BWD 0.0529, which meant that BWD exhibited better sensitivity to small shifts in the process it monitored. This is an indication, as a whole, that procedures based on Bayesian theory present better control performance with smaller control limits and less variability.

Table 9. Control Chart Parameters for Newborns' Body Temperature

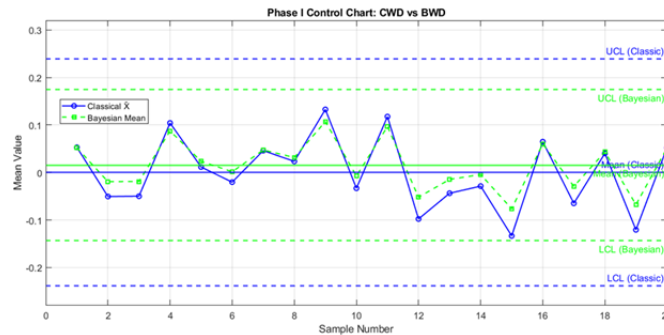| Chart	UCL	LCL	Target	Sigma	CLW
Classical	37.4110	36.5690	36.9900	0.1403	0.8421
Bayesian	37.2134	36.7107	36.9621	0.0838	0.5027
CWA	37.3367	36.6433	36.9900	0.1156	0.6933
BWA	37.1569	36.7672	36.9621	0.0650	0.3897
CWD	0.2390	-0.2390	0.0000	0.0797	0.4779
BWD	0.1743	-0.1432	0.0155	0.0529	0.3175

Figure 10. CWD and BW Charts for Body Temperatures of Newborns (Phase II).

5. Conclusion

It was concluded from simulation experiments that:
1. This study successfully compared classical and Bayesian control charts for monitoring the process mean, utilizing wavelet-based methods for both the approximation and detail sub-bands.
2. Bayesian control charts were generally more efficient as they resulted in narrower control limits, lower estimates of process variability, and higher sensitivity to the identification of small and medium mean shifts in the process.

3. The integration of wavelet decomposition notably improved the detection capability of both classical and Bayesian control charts, particularly in the detail domain where high-frequency process variations are captured.

4. Among the evaluated charts, the Bayesian Wavelet Approximation (BWA) and Bayesian Wavelet Detail (BWD) charts exhibited the smallest control limit widths, the most desirable Average Run Length (ARL) values, enhancing their practicality for high-precision monitoring.

5. The strength of prior information in Bayesian charts significantly affected performance; strong informative priors resulted in better detection ability and more stable ARL values, non-informative priors made Bayesian performance converge with classical charts and confirmed the flexibility of the Bayesian framework.

From the practical application of the data, the following conclusions were drawn:

1. The wavelet-enhanced control charts, particularly the Bayesian-based BWA and BWD charts, demonstrated superior performance compared to classical Shewhart and standard Bayesian charts.

2. The Bayesian wavelet charts showed reduced variability and tighter control limits, reflecting higher precision in monitoring newborn body temperatures.

3. The wavelet-enhanced charts were more sensitive to minor shifts in the monitored process, crucial for early detection in neonatal healthcare.

4. The Bayesian approach, incorporating prior information and updating with each new observation, significantly improved monitoring accuracy.

5. The study underscores the importance of advanced control chart methods in neonatal care, where early identification of temperature deviations is vital to patient health.

6. Recommendations

1. The findings recommend the Bayesian wavelet-based approach as a reliable and efficient method for modern process control, especially where quick and accurate detection of subtle process changes is critical.

2. Future extensions could involve applying this hybrid control charting methodology to multivariate processes, incorporating robust estimation techniques, and exploring real-life healthcare and industrial applications.

Appendix

Table 10. Body Temperatures of Newborn Infants for Phase I

Sample	X_1	X_2	X_3	X_4	X_5	Mean	S. D.
1	36.60	37.20	36.80	37.30	36.70	36.92	0.2598
2	37.00	36.90	37.10	36.60	37.10	36.94	0.2062
3	36.90	36.90	36.80	36.50	36.80	36.78	0.1732
4	37.20	36.60	36.80	37.50	36.60	36.94	0.3811
5	37.10	37.00	37.50	36.80	36.90	37.06	0.2640
6	36.60	36.80	37.20	37.00	36.80	36.88	0.2291
7	37.30	37.20	36.90	36.70	37.50	37.12	0.3202
8	37.20	37.40	37.00	37.50	37.10	37.24	0.1924
9	37.40	37.50	37.40	36.70	36.80	37.16	0.3753
10	36.70	37.50	36.70	36.80	37.40	37.02	0.3429
11	37.10	37.50	36.70	36.60	37.20	37.02	0.3640
12	37.50	36.90	36.60	36.60	37.30	36.98	0.3821
13	37.40	36.90	36.60	36.50	37.40	36.96	0.3997
14	36.70	36.70	37.20	37.00	36.80	36.88	0.2082
15	36.70	37.50	37.20	37.50	37.10	37.20	0.3420
16	37.30	36.90	36.70	37.40	36.70	37.00	0.3197
17	37.10	37.20	36.60	37.00	36.60	36.90	0.2784
18	37.40	36.80	36.60	36.70	36.60	36.82	0.3162
19	37.20	36.60	36.90	37.30	37.20	37.04	0.2625
20	37.30	36.90	36.60	37.40	36.50	36.94	0.3708

Table 11. Body Temperatures of Newborn Infants for Phase II

Sample	X_1	X_2	X_3	X_4	X_5	Mean	S. D.
1	37.10	37.00	37.50	36.80	36.90	37.06	0.2772
2	37.30	37.20	36.90	36.70	37.50	37.12	0.2799
3	37.40	37.50	37.40	36.70	36.80	37.16	0.2753
4	37.10	37.50	36.70	36.60	37.20	37.02	0.2890
5	37.40	36.90	36.60	36.50	37.40	36.96	0.3266
6	36.70	37.50	37.20	37.50	37.10	37.20	0.2857
7	37.10	37.20	36.60	37.00	36.60	36.90	0.2692
8	37.20	36.60	36.90	37.30	37.20	37.04	0.2772
9	37.00	36.90	37.10	36.60	37.10	36.94	0.2048
10	37.20	36.60	36.80	37.50	36.60	36.94	0.3266
11	36.60	36.80	37.20	37.00	36.80	36.88	0.2332
12	37.20	37.40	37.00	37.50	37.10	37.24	0.2184
13	36.70	37.50	36.70	36.80	37.40	37.02	0.2704
14	37.50	36.90	36.60	36.60	37.30	36.98	0.2904
15	36.70	36.70	37.20	37.00	36.80	36.88	0.1976
16	37.30	36.90	36.70	37.40	36.70	37.00	0.2704
17	37.40	36.80	36.60	36.70	36.60	36.82	0.2801
18	37.30	36.90	36.60	37.40	36.50	36.94	0.3023

REFERENCES

1. Ali, Taha Hussein and Rahim, Alan Ghafur and Saleh, Dlshad Mahmood, *Construction of bivariate f-control chart with application*, Eurasian Journal of Science and Engineering, vol. 4, no. 2, pp. 116–133, 2018.
2. Antony, Jiju and Viles, Elisabeth and Torres, Alexandre Fonseca and Fernandes, Marcelo Machado and Cudney, Elizabeth A, *Design of experiments in the service industry: results from a global survey and directions for further research*, The TQM Journal, vol.33, no. 5, pp. 987–1000, 2021.
3. Lin, Chien-Hua and Lu, Ming-Che and Yang, Su-Fen and Lee, Ming-Yung, *A Bayesian control chart for monitoring process variance*, Applied Sciences, vol.11, no. 6, pp. 2729, 2021.
4. Majeed, Rasheed and Haddar, Maroua and Chaari, Fakher and Haddar, Mohamed, *A wavelet-based statistical control chart approach for monitoring and detection of spur gear system faults*, International Conference on Acoustics and Vibration, pp. 140–152, 2022.
5. Khan, Imad and Khan, Dost Muhammad and Noor-ul-Amin, Muhammad and Khalil, Umair and Alshanbari, Huda M and Ahmad, Zubair, *Hybrid EWMA control chart under bayesian approach using ranked set sampling schemes with applications to hard-bake process*, Applied Sciences, vol.13, no. 5, pp. 2837, 2023.
6. Bayer, Fábio M and Kozakevicius, Alice J and Cintra, Renato J, *An iterative wavelet threshold for signal denoising*, Signal Processing, vol.162, pp. 10–20, 2019.
7. Supharakonsakun, Yadpirun, *Bayesian Control Chart for Number of Defects in Production Quality Control*, Mathematics, vol.12, no. 12, pp. 1903, 2024.
8. Percival, Donald B and Walden, Andrew T, *Wavelet methods for time series analysis*, Cambridge university press, vol.4, 2000.
9. Alkhateeb, Ahmed Naziyah and Al-Qazaz, Qutaiba N Nayef, *Variable Selection in Weibull Accelerated Survival Model Based on Chaotic Sand Cat Swarm Algorithm*, Statistics, Optimization & Information Computing, vol.13, no. 5, pp. 2105–2118, 2025.
10. Montgomery, Douglas C, *Introduction to statistical quality control*, John wiley & sons, 2020 .
11. Al-hashimi, Muzahem Mohammed and Alkhateeb, Ahmed Naziyah, *Spatial analysis of brain and other cns cancers incidence in Iraq during 2000-2015*, Malaysian Journal of Public Health Medicine, vol.20, no. 3, pp. 27–34, 2020 .
12. Ali, Taha Hussein and Sedeeq, Bekhal Samad and Saleh, Dlshad Mahmood and Rahim, Alan Ghafur, *Robust multivariate quality control charts for enhanced variability monitoring*, Quality and Reliability Engineering International, vol.40, no. 3, pp. 1369–1381, 2024.
13. Ali, Taha Hussein and Haydier, Esraa Awni, *Using Wavelet in constructing some of Average Charts for Quality control with application on Cubic Concrete in Erbil*, Polytechnic Journal, vol.6, pp. 171–209, 2016.
14. Gelman, Andrew and Carlin, John B and Stern, Hal S and Rubin, Donald B, *Bayesian data analysis*, Chapman and Hall/CRC, 1995 .
15. Woodall, William H and Montgomery, Douglas C, *Research issues and ideas in statistical process control*, Journal of Quality Technology, vol.31, no. 4, pp. 376–386, 1999.
16. Ali, Mohamed ,Taha, Hutheyfa Hazem, *Application of RBF neural network in predicting thalassemia disease in Mosul city* , Statistics, Optimization and Information Computing, vol.14, no. 1, pp. 229–246, 2025.
17. Hasan, M. T., Ali, T. H., and Kareem, N. H. S., *Multivariate CUSUM Daubechies Discrete Wavelet Transformation Coefficients Charts for Quality Control*, Passer Journal of Basic and Applied Sciences, vol. 7, no. 1, pp. 533–546, 2025.
18. Elias, I. Ibrahim and Ali, T. Hussein, *VARMA Time Series Model Analysis Using Discrete Wavelet Transformation Coefficients for Coiflets Wavelet*, Passer Journal of Basic and Applied Sciences, vol. 7, no. 2, pp. 657–677, 2025.
19. Hasawy, M. Abduljabar Ibrahim, Ali, T. H., and Sedeeq, B. S., *Fast MCD-Augmented Rank Regression for Robust Estimation of Weibull Parameters*, Passer Journal of Basic and Applied Sciences, vol. 7, no. 2, pp. 689–697, 2025.
20. Taher, M., Al-Hasso, T. A.-R. S., and Ali, T. H., *A Novel Dmey Wavelet Charts for Controlling and Monitoring the Average and Variance of Quality Characteristics*, Statistics, Optimization & Information Computing, 2025.

21.   Omer, A. Wali and Ali, T. Hussein, *Wavelet Analysis for Outlier Estimation in Multivariate Linear Regression Models*, Passer Journal of Basic and Applied Sciences, vol. 7, no. 1, pp. 478–494, 2025.

22.   Hayawi, H. A., Azeez, S. M., Babakr, S. O., and Ali, T. H., *ARX Time Series Model Analysis with Wavelets Shrinkage (Simulation Study)*, Pakistan Journal of Statistics, vol. 41, no. 2, pp. 103–116, 2025.

23.   Ali, T. H., Hamad, A. A., Mahmood, S. H., and Ahmed, K. H., *ARIMAX Time Series Analysis for a General Budget in the Kurdistan Region of Iraq Using Wavelet Shrinkage*, Communications in Statistics: Case Studies, Data Analysis and Applications, vol. 11, no. 2, pp. 164–188, 2025.

24.   Al-Hashimi, M., Hayawi, H., and Alawjar, M., *Ensemble Method for Intervention Analysis to Predict the Water Resources of the Tigris River*, Statistics, Optimization and Information Computing, vol. 14, pp. 144–161, 2025.

25.   Botani, D., Kareem, N., Ali, T., and Sedeeq, B., *Optimizing Bandwidth Parameter Estimation for Non-Parametric Regression Using Fixed-Form Threshold with Dmey and Coiflet Wavelets*, Hacettepe Journal of Mathematics and Statistics, vol. 54, no. 3, pp. 1094–1106, 2025.

26.   Hayawi, H., Al-Hashimi, M., and Alawjar, M., *Machine Learning Methods for Modelling and Predicting Dust Storms in Iraq*, Statistics, Optimization and Information Computing, vol. 13, no. 3, pp. 1063–1075, 2025.

27.   Ali, T. H., Hayawi, H. A.-M., and Botani, D. S. I., *Estimation of the Bandwidth Parameter in Nadaraya-Watson Kernel Non-Parametric Regression Based on Universal Threshold Level*, Communications in Statistics - Simulation and Computation, vol. 52, no. 4, pp. 1476–1489, 2023.

28.   Shakir, Yousif Ali and Taha, Hutheyfa Hazem, *Build fuzzy model with conditional rules with the application*, AIP Conference Proceedings, vol. 2834, no. 1, pp. 080125, 2023.

29.   Alkhateeb, Ahmed Naziyah and Algamal, Zakariya Yahya, *Variable selection in gamma regression model using chaotic firefly algorithm with application in chemometrics*, Electronic Journal of Applied Statistical Analysis, vol. 14, no. 1, pp. 266–276, 2021.

30.   Tareq Hasan, Marwan H and Ali, Taha H and Sedeek Kareem, Nazeera H, *Multivariate CUSUM Daubechies Discrete Wavelet Transformation Coefficients Charts for Quality Control*, Passer Journal of Basic and Applied Sciences, vol. 7, no. 1, pp. 533–546, 2025.